Significance of Gamma-ray Detector Efficiency Calibration Bias on Nuclear Astrophysics and Nuclear Data Evaluations

Eric F. Matthews[a,*], Amanda M. Lewis[a], Lee A. Bernstein[a,b]

[a] *Department of Nuclear Engineering, University of California, Berkeley, California 94720 USA*
[b] *Nuclear Science Division, Lawrence Berkeley National Laboratory, Berkeley, California 94720 USA*

Abstract

The use of a canonical logarithmic polynomial γ-ray efficiency calibration form results in significant biases in efficiency for both interpolated and extrapolated γ-ray energies. The effects of this bias are explored and are shown to present a pervasive problem. A comparison of efficiency calibrations for a standard HPGe detector using a physically-informed model and the canonical logarithmic polynomial form is presented. Statistical analyses are performed on a calibration dataset to demonstrate significant oscillations in the efficiency curve when the logarithmic polynomial form is used, highlighting that this form cannot be reliably used for interpolation. A review of standard γ-ray spectroscopy software packages is presented, showing widespread use of the logarithmic polynomial form for efficiency calibrations. This is followed by a review of both the high-energy ^{66}Ga calibration standard and measurements of the ^{12}C(α,γ) reaction. The bias introduced through the use of the logarithmic polynomial calibration is wide-ranging, influencing calibration methods and standards, nuclear structure evaluations, nuclear structure and reaction measurements, nuclear forensics analyses, radioisotope production, and nuclear astrophysical models. It is concluded that physically-informed models of energy-dependent photopeak efficiency should be used in future measurements of nuclear properties.

Keywords: efficiency calibration, efficiency bias, efficiency uncertainty

1. Motivation

Proper energy-dependent efficiency calibration of γ-ray detectors is a critical task in many nuclear measurements. A careful treatment of energy-dependent efficiency calibration is required to avoid biasing both extrapolated and interpolated efficiency values. In this paper it is shown that an alarming portion of nuclear data measurements have been performed using a logarithmic polynomial calibration curve that has no

*Corresponding author
Email address: efmatthews@berkeley.edu (Eric F. Matthews)

physical basis and can result in erroneous efficiency values for γ-ray energies far from discrete lines in the calibration sources used.

The structure of this article is as follows. Sections 2.1 and 2.2 detail two methods of fitting functional forms to empirical data: physically-informed models and the canonical logarithmic polynomial formulation. Section 2.3 discusses Monte-Carlo simulation of energy-dependent detector efficiency using standard software packages as an alternative method of efficiency calibration. Section 3 uses an experimental dataset to demonstrate the bias inherent in logarithmic polynomials as compared to physically-informed models for both extrapolated and interpolated values. Section 4 presents a literature review that demonstrates widespread use of non-physical efficiency calibrations in standard γ-spectroscopy software. Sections 4.1, 4.2, and 4.3 offer reviews of the HYPERMET γ spectroscopy package, a ^{66}Ga calibration standard, and measurements of γ-ray data relevant to the astrophysically-important ^{12}C(α,γ) reaction, respectively. These reviews demonstrate the potential propagation of efficiency calibration bias through a number of publications on calibration methods and standards, nuclear structure evaluations, nuclear structure and reaction measurements, nuclear forensics analyses, radioisotope production, and nuclear astrophysical constants.

2. Efficiency Calibration Methods

Energy-dependent photopeak efficiency calibration of γ-ray detectors can generally be categorized into two methodologies: fitting functional forms to empirical data and Monte-Carlo simulation. Sections 2.1 and 2.2 detail two methods for fitting functional forms to empirical data, while Sec. 2.3 briefly discusses Monte-Carlo simulation.

2.1. Logarithmic Polynomials

Logarithmic polynomials have served as a staple of energy-dependent γ-ray efficiency calibration. The use of logarithmic polynomials has been widely promoted in popular educational materials [1, p. 458], research literature [2, 3], and γ-spectroscopy software [4, 5, 6, 7, 8, 9]. This widespread use is primarily due to the ease with which these forms can be fitted using linear regression methods to obtain an analytical fit. The ease of use of this functional form has been noted in literature [2]. Equation 1 offers an example of a commonly-used fifth-order logarithmic polynomial efficiency calibration fit:

$$\begin{gathered}\varepsilon(E_\gamma) = B_0 + B_1 ln(E_\gamma) + \\ B_2 ln(E_\gamma)^2 + B_3 ln(E_\gamma)^3 + B_4 ln(E_\gamma)^4\end{gathered} \tag{1}$$

where $\varepsilon(E_\gamma)$ is the absolute photopeak efficiency of the detector for photopeak detection of γ rays with energy E_γ and B_0 through B_4 are the polynomial coefficients that have no physical interpretation.

2.2. Physical Formulations

Several non-linear functional forms exist that represent the expected energy-dependent behavior of a γ-ray detector. The analysis presented in Sec. 3 focuses on the physically-informed model of energy-dependent γ-ray efficiency presented in Eq. 2 (although a number of related models exist in literature). This model was originally presented by Gallagher and Cipolla [10] for the purpose of efficiency calibration of Si(Li) X-ray detectors. However, this model is generally applicable to any photopeak detector with either a dead-layer or non-active entrance window. The form of this model is:

$$\varepsilon(E_\gamma) = B_0\, e^{-B_1 E_\gamma^{B_2}} (1 - e^{-B_3 E_\gamma^{B4}}) \tag{2}$$

where B_0 represents a geometric efficiency scalar term, and the $(1-e^{-B_3 E_\gamma^{B4}})$ term represents the probability of the gamma-ray penetrating the detector dead-layer, and $e^{-B_1 E_\gamma^{B_2}}$ represents the probability of interaction inside the detector volume. The $B_1 E_\gamma^{B_2}$ and $B_3 E_\gamma^{B4}$ terms represent the energy-dependent attenuation coefficients of the detector and dead layer, respectively.

When efficiency data are not available below the expected turn-around in the γ-ray efficiency curve, Eq. 2 can be modified to the form in Eq. 3 which removes the term for dead-layer attenuation, $e^{-B_1 E_\gamma^{B_2}}$, as that term becomes unity above the turn-around.

$$\varepsilon(E_\gamma) = B_0\, e^{-B_1 E_\gamma^{B_2}} \tag{3}$$

The practical barrier to the use of non-linear physically-informed efficiency models has been the difficulty in performing a global minimization that yields the best fit. However, as new computational methods and data analysis software have become available there is no longer any need to use the logarithmic polynomial form. The authors recommend the use of metaheuristic minimization methods, namely the differential evolution method [11] which has been implemented in the Python numerical analysis package SciPy [12].

It should be noted that any model used for energy-dependent efficiency calibration must be selected carefully given the particular efficiency dataset and the energy region where efficiency values will be calculated. There should be measured efficiency values for each region of the efficiency calibration. Moreover, the model that is used should describe all of the expected energy-dependent behavior within the region of interest. For example, the physical form given in Eq. 2 is only applicable from energies just above the K-shell X-ray edge of the detector material to the energy where pair production begins to compete with Compton scattering. For common HPGe detector geometries, these two boundaries are approximately 20 keV [1, p. 453] and 2-3 MeV [1, p. 439], respectively. At energies when pair production becomes significant, the terms B_1 and B_2 in Eq. 2 will exhibit an energy dependence and thus the model given by Eq. 2 would no longer be applicable. Equation 2 is sufficient for the energy range of the dataset used in this study; however, it is not the only physical model of energy-dependent efficiency available and a different dataset with a wider range of efficiency data would likely need an enhanced model.

2.3. Monte-Carlo Simulation

Monte-Carlo simulations can be used to assess the probability of a full-energy deposition in the extended geometry of that detector. This method simulates a large number of randomly sampled photon interaction tracks within the detector and its environment in order to assess bulk quantities of the detection system. Such a method can be facilitated by standard Monte-Carlo physics packages including GEANT and MCNP [13].

Monte-Carlo simulations require accurate and detailed knowledge of the geometry of both the detector apparatus and the source. However, Monte-Carlo simulation can prove useful in modeling source geometries and self-attenuation factors that may not be possible with standard efficiency calibration measurements. The efficiency calculated using a physically-accurate Monte Carlo simulation will not directly exhibit the issues associated with the logarithmic polynomial approach, but if it is normalized against a calibration that employs the logarithmic polynomial formalism it could produce spurious results. Further review of Monte-Carlo efficiency calibrations can be found in literature and the authors point to Reference [13] in particular.

Table 1: Efficiency obtained from calibration source spectrum.

γ Energy (keV)	Source	Abs. Efficiency (%)
59.5409	^{241}Am	0.00124(3)
121.7817	^{152}Eu	0.00372(3)
244.6974	^{152}Eu	0.00206(4)
302.0129	^{133}Ba	0.00168(3)
344.2785	^{152}Eu	0.00138(2)
356.0192	^{133}Ba	0.001282(8)
383.8485	^{133}Ba	0.00121(3)
411.1165	^{152}Eu	0.00010(2)
443.9606	^{152}Eu	0.0011(1)
661.657	^{137}Cs	0.000605(5)
778.9045	^{152}Eu	0.00049(1)
867.38	^{152}Eu	0.00040(4)
964.057	^{152}Eu	0.000373(8)
1085.837	^{152}Eu	0.00034(3)
1112.076	^{152}Eu	0.00032(1)
1173.228	^{60}Co	0.000310(4)
1212.948	^{152}Eu	0.00031(5)
1299.142	^{152}Eu	0.00033(4)
1332.492	^{60}Co	0.000272(1)
1408.013	^{152}Eu	0.00025(2)
1528.1	^{152}Eu	0.0002(3)

3. Comparison of Efficiency Calibrations

In order to demonstrate the bias introduced by the use of a logarithmic polynomial form for efficiency calibration, a set of experimental efficiency data was analyzed. These data were obtained from a calibration spectrum that was collected on a Model IGC-13 HPGe from Princeton Gamma Technology. Five calibration sources were used to generate this spectrum: ^{133}Ba, ^{241}Am, ^{137}Cs, ^{152}Eu, and ^{60}Co. These sources were placed at a standoff distance of approximately one meter in order to eliminate coincidence summing effects. These data were collected over four days from January 11 to 14, 2019. Twenty-one photopeaks from these calibration sources were successfully fit in order to obtain the net counts in each photopeak. Table 1 details the efficiency data obtained from each photopeak.

Equations 1 and 2 were fit to this efficiency data. Monte-Carlo uncertainty propagation [14] was used to obtain a covariance matrix for the parameters of each fit and to calculate the uncertainty envelope. This uncertainty propagation method is necessary as both functional forms are highly non-linear and thus the linear uncertainty propagation formula is not applicable. The complete and annotated analysis for this dataset has been preserved in Reference [15].

The fit obtained using the data in Tbl. 1 and logarithmic polynomial formulation in Eq. 1 is shown in Fig. 1. The fit obtained using the data in Tbl. 1 and the physical model in Eq. 2 is shown in Fig. 2. Within

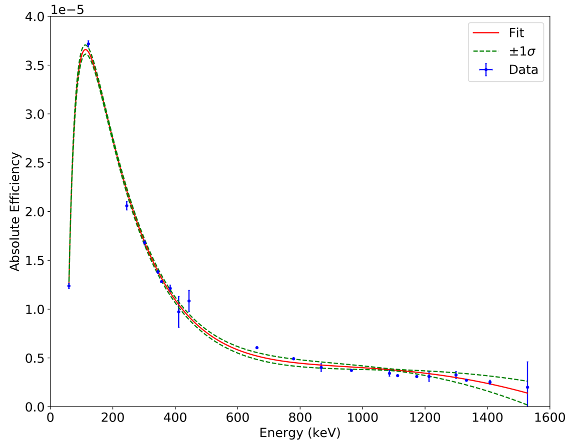

Figure 1: Logarithmic polynomial efficiency curve obtained using the data in Tbl. 1 and Eq. 1. The Pearson χ^2 value of this fit is 1.1×10^{-6}.

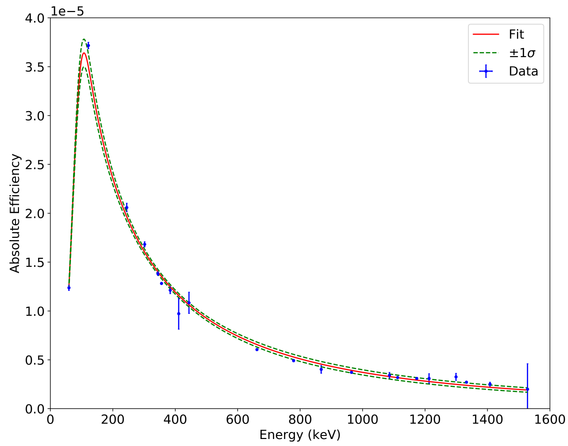

Figure 2: Physically-informed efficiency curve obtained using the data in Tbl. 1 and Eq. 2. The Pearson χ^2 value of this fit is 1.1×10^{-6}.

the energy region of the efficiency data in Tbl. 1, both fits appear visually to be reasonable, each with Pearson χ^2 values of 1.1×10^{-6}. However, Fig. 3, which shows the percent difference between the energy curves in Figs. 1 and 2, reveals that there are drastic differences between these two curves across the energy range of the experimental data; the curves disagree by over 20% at several points across the domain of the efficiency data. The following two subsections detail a series of tests on the two curves in order to determine which functional form yields a valid efficiency calibration.

3.1. Extrapolation

A simple test of the ability of each functional form to accurately predict extrapolated efficiency values was performed. Efficiency values above 1200 keV were removed from the dataset presented in Tbl. 1 and

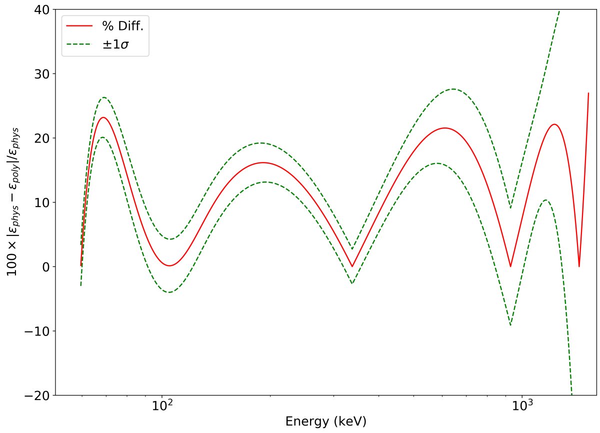

Figure 3: Percent difference between the efficiency curves displayed in Figs. 2 and 1 as a function of energy. The uncertainty envelope around this line was obtained using the linear uncertainty propagation formula. The x-axis is shown in logarithmic scale in order to reveal more detail.

both the physical model and the logarithmic polynomial were fit to this subset of the data in order to test the ability of each approach to extrapolate the efficiency to higher energies. A comparison to the data points not included in the fits (those above 1200 keV) can be seen in Fig. 4. The fit to the logarithmic polynomial in Eq. 1 significantly underpredicts the efficiency data points above 1200 keV. This is not surprising as the logarithmic polynomial form has no physical basis to guide extrapolation. The fit to the physical model with efficiency data points below 1200 keV is markedly more reasonable. The fits to the physical model with and without data points above 1200 keV underpredict the experimental efficiency values, but in both cases, the physical model clearly provides a more realistic energy-dependent description of the efficiency curve. Caution should be used when extrapolating any fit beyond the domain of the underlying data; however, this example clearly demonstrates that the logarithmic polynomial form cannot be used for extrapolation as it fails to capture both the magnitude and shape of the efficiency curve beyond the domain of the data.

3.2. Deleted Residual Analysis

Deleted residual analysis was performed in order to demonstrate bias due to oscillations that result from using different subsets of the efficiency data. The method of deleted residual analysis involves deleting one data point from the dataset, refitting the model on the remaining $n - 1$ observations, and observing the effects of this deletion [16, p. 283]. This simulates the change in residuals that would result when an experimentalist has a constrained set of efficiency data. Figures 5a and 5b display the resulting fits to Eq. 1 and 2, respectively, when one efficiency data point is removed from the dataset in Tbl. 1 at a time. The fit to the logarithmic polynomial efficiency calibration exhibits far greater modulation between the remaining

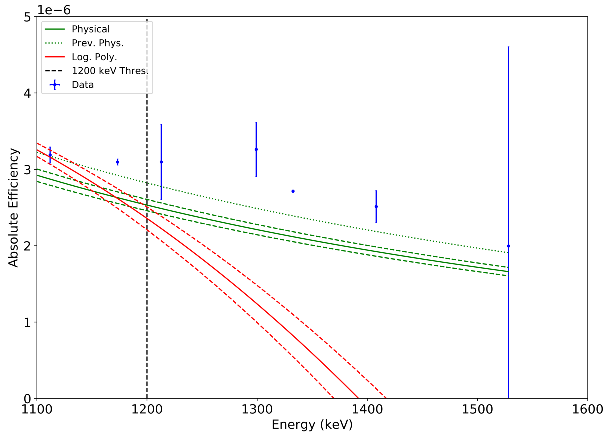

Figure 4: Efficiency calibrations at energies above 1150 keV. The dotted green line is the fit obtained using the physical model in Eq. 2 using all of the data in Tbl. 1. The solid green line with dashed uncertainty bands is the fit obtained using the physical model with data points from Tbl. 1 that have energies below 1200 keV. The solid red line with dashed uncertainty bands is the fit obtained with the logarithmic polynomial in Eq. 1 with data points from Tbl. 1 that have energies below 1200 keV. It can be seen that the logarithmic polynomial cannot be used for extrapolation, while the physical model preserves the energy-dependent shape of the curve when extrapolated.

data points than the physical form. These variations introduce an interpolation bias, particularly in energy regions where there are no efficiency data points present to guide the fit. One would expect that these variations would be even larger had all the data points from particular calibration sources, such as ^{60}Co or ^{133}Ba, been removed. Such would represent the oscillations that would occur when an experimentalist had only a subset of the five calibration sources used in this experiment; indeed it is often the case that calibrations are performed with only one or two multi-line sources.

In this example, this effect is particularly large in the 220 keV gap between the 443.9606 keV and 661.657 keV data points. Figure 6 shows Fig. 5 zoomed to this region. The oscillations that result from the use of the logarithmic polynomial are large, whereas the physical model offers consistent results. For example, at the 511 keV positron-electron annihilation peak, the standard deviation in the fits resulting from the logarithmic polynomial form is 2.3×10^{-7}, while the physical model is a factor of over five less at 4.3×10^{-8}. The range of efficiency values obtained from the logarithmic polynomial fit at 511 keV is 14.1% about their mean, whereas for the physical model this is only 2.4%. This demonstrates the superiority of the physical model over the logarithmic polynomial form for energies interpolated between the measured data points, as well as those extrapolated above them as shown in Sec. 3.1.

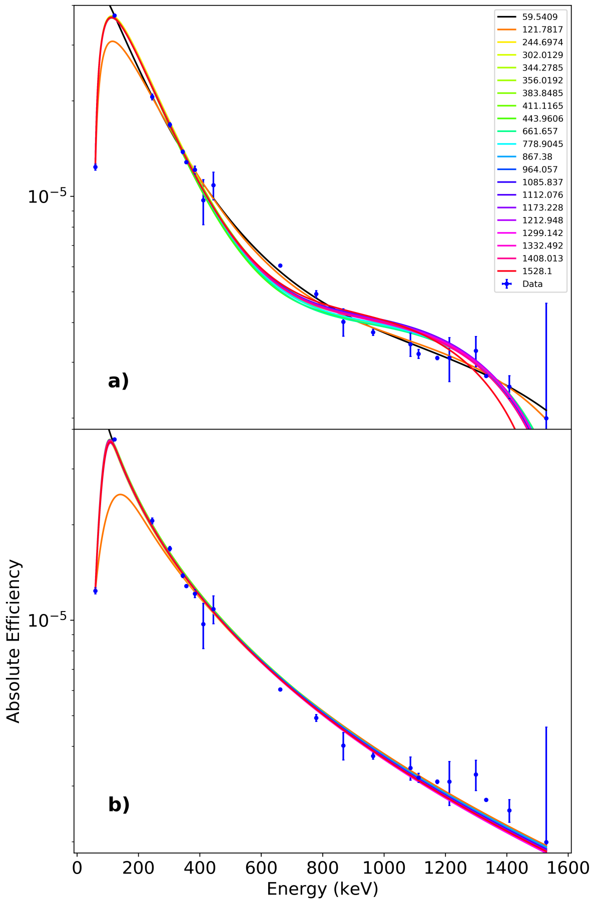

Figure 5: a) Deleted residual analysis performed using the efficiency data in Tbl. 1 and fit to the logarithmic polynomial form in Eq. 1. b) Deleted residual analysis fit to the physically-informed model in Eq. 2. The color-coded legend indicates which efficiency data point in Tbl. 1 was excluded when obtaining that particular fit.

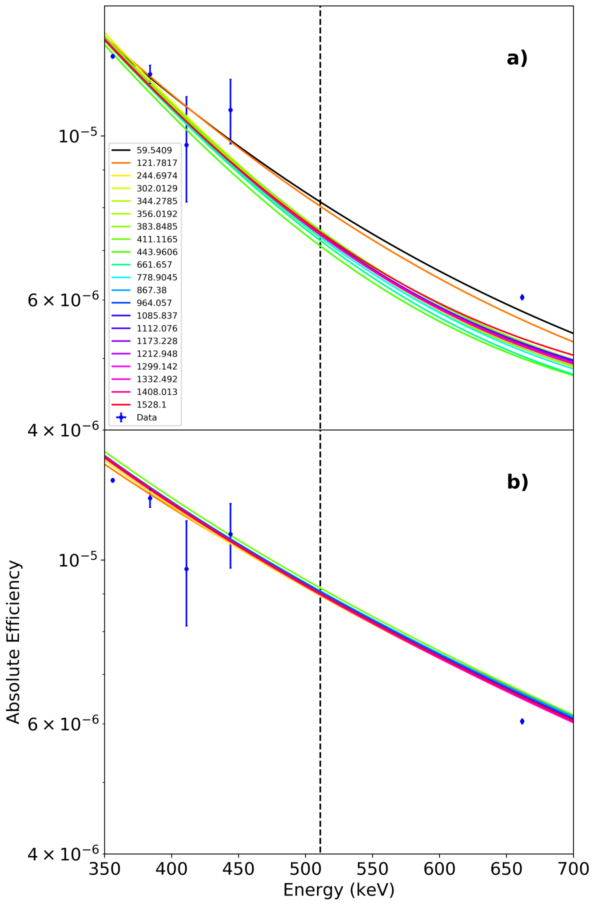

Figure 6: Figure 5 zoomed between 350 and 700 keV. The black dashed line is located at 511 keV, the energy of commonly measured annihilation photons. It can be seen that the results of the physical model shown in panel b) provide significantly improved consistency in this region of limited empirical data when compared to the results obtained from the logarithmic polynomial shown in panel a).

4. Review of Literature on Measurements, Standards, and Methods

The logarithmic polynomial efficiency form has been widely employed in standard γ-spectroscopy software packages due to its ease of use and analytical regression, including RadWare [4], SAMPO [5, 6], GAMANAL [7, 8], and HYPERMET [9]. Furthermore, many published results do not provide sufficient detail about the steps taken to obtain their efficiency calibrations to allow a good understanding of their attendant uncertainties. Presumably in some of these cases this lack of detail is because it is trusted that a reasonable treatment can be obtained through standard spectroscopy software packages. Both of these issues will be discussed in the following sections.

4.1. HYPERMET

HYPERMET is a γ-spectroscopy package that features automated peak fitting and detector energy, efficiency, and non-linearity calibrations [9]. This code package has been used for a number of γ-spectroscopy measurements and applications, as evidenced by the 110 citations tabulated by Google Scholar for the HYPERMET publication [9] as of November 11, 2019. Seventy of these citations were reviewed and of these, 18 were identified that either explicitly mentioned the use of the HYPERMET efficiency calibration tool or made use of the logarithmic polynomial functional form used by HYPERMET. These citations include five papers on calibration methods/standards [2, 17, 18, 19, 3], six on prompt gamma and neutron activation analyses [20, 21, 22, 23, 24, 25], three on nuclear structure measurements [2, 19, 3], five on nuclear reaction measurements [26, 27, 28, 29, 30], and two on gamma spectroscopy software [31, 32]. These 18 papers have a collective total of 705 citations according to Google Scholar as of November 11, 2019. This demonstrates the broad impact of HYPERMET and potential propagation of the bias introduced by logarithmic polynomial efficiency calibration. Section 4.2 will detail the broader impacts of the use of the logarithmic polynomial in HYPERMET on a widely used ^{66}Ga calibration standard that is established in Reference [3].

4.2. ^{66}Ga Calibration Standard

A measurement of the intensities of decay γ rays from ^{66}Ga ($t_{1/2}$ = 9.49(3) h) was used to develop a high-energy calibration standard for HPGe detectors [3]. ^{66}Ga is particularly useful for this purpose due to its strong transitions at 2189.616 keV and 4295.224 keV. The measurement employed HYPERMET in order to perform the efficiency calibration of the HPGe detector used. The sources used in this calibration included ^{56}Co which emits γ rays up to 3451 keV and a ^{13}C(^{238}Pu) source which produced a single high-energy γ ray at 6129 keV via the ^{13}C(α,n) reaction. This leaves a 2678 keV gap with no efficiency data points to guide the logarithmic polynomial efficiency curve obtained from HYPERMET. The 3791.036 keV, 4085.853 keV, 4295.224 keV, and 4806.007 keV γ rays evaluated in the measurement all fall within this gap. Similarly, the 2189.616 keV and 2422.525 keV γ rays sit in another 500 keV gap in the efficiency data. As was demonstrated in Sec. 3.2, even a gap of 200 keV in the data used to fit the logarthmic polynomial form can result in significant interpolation bias in the resulting efficiency calibration. The example in Sec. 3.2 features 21 efficiency data points over a range of 1400 keV, whereas this standard measurement has a significantly lower density of efficiency data with 36 efficiency data points over 6100 keV. This means interpolation bias will likely be present in this measurement and the resulting calibration standard.

A review of the citations of this calibration standard was performed. Twenty-four of these citations were reviewed and categorized. They include nine papers on calibration methods/standards [2, 33, 18, 19, 34, 35, 36, 37, 38], nine on nuclear structure and decay measurements [19, 39, 40, 41, 42, 43, 44, 45, 46], five on nuclear reaction measurements [47, 48, 49, 42, 43], two nuclear structure evaluations [50, 51], and two papers on radioisotope production [52, 53]. These citations are secondary citations to the HYPERMET publication [9] and have 609 citations of their own according to Google Scholar as of November 11, 2019. These 609 citations are in turn ternary citations of the HYPERMET paper, demonstrating the impact of logarithmic polynomial efficiency calibrations throughout published literature.

4.3. Review of ^{12}C(α,γ) Measurements

A review of the possible impact of efficiency calibration bias on a key reaction of interest to nuclear astrophysics, ^{12}C(α,γ), was performed. This reaction rate is particularly susceptible to bias in the extrapolated high-energy γ-ray efficiency calibrations since it proceeds through the emission of 6-9+ MeV transitions in ^{16}O. The measurements that form the basis of the NACRE-II evaluation for this reaction [54] were reviewed and the method by which each measurement performed its efficiency calibration was tabulated. Sixteen measurements are cited in the evaluation, of which 15 used γ spectroscopy as a part of the measurement. These measurements included photopeak measurements with HPGe [55, 56, 57, 58, 59, 60, 61, 62], NaI [63, 55, 64, 65, 66, 67], BaF_2 [68], and BGO [69] detectors. Of these 15 measurements, three used Monte-Carlo simulations to perform their calibrations [64, 58, 69], one used a logarithmic polynomial [63], and 11 did not provide sufficient detail to make any conclusions about the method of the calibration or cited efficiency calibrations in literature that were not publicly available [55, 56, 57, 59, 60, 61, 62, 55, 65, 66, 67, 68]. Of the measurements that did detail their efficiency calibration sufficiently, 25% used a logarithmic polynomial form. More concerningly, 73% of the measurements that comprise the evaluation did not sufficiently detail their efficiency calibration in literature to allow for determination of the efficiency method used. This lack of detail may be due to the use of standard γ-spectroscopy software for efficiency calibrations which use logarithmic polynomials in efficiency calibration. It is quite likely that some of those 11 measurements lacking sufficient details were affected by bias in their efficiency calibration.

5. Conclusion

This study has demonstrated the importance of careful selection of efficiency calibration functional forms. In particular, it has been shown that physically-informed models of energy-dependent efficiency should be used. In comparison to the canonical logarithmic polynomial, physical efficiency models provide better fidelity when obtaining extrapolated values and avoid biasing of interpolated values. The logarithmic polynomial form allows for ease of use due to its analytical regression methods. However, with modern mathematical methods and software packages there is no longer a need to continue the use of logarithmic polynomial function forms. Due to the issues with the logarithmic polynomial that have been demonstrated in this study, it is encouraged that the γ spectroscopy community start using the more physical model for detector efficiency and γ-spectroscopy packages should be updated to use physical models.

A review of research literature has revealed a widespread use of the logarithmic polynomial for detector efficiency calibration, including four major γ-spectroscopy packages. A review of the publications that use the HYPERMET γ-spectroscopy software package [9] showed 705 cases throughout nuclear structure and reaction studies which could have been impacted by the use of the logarithmic polynomial form for the efficiency calibration. One of these citations [3], established ^{66}Ga as a high-energy calibration standard. Twenty-four publications cite this standard, propagating potential bias forward into calibration methods/standards, nuclear structure and reaction measurements, nuclear structure evaluations, and radioisotope production. In addition to the issues stemming from the use of the logarithmic polynomial efficiency form, a review of measurements of the astrophysically-significant ^{12}C(α,γ) reaction shows that an overwhelming majority of peer-reviewed publications on these measurements do not provide sufficient detail to determine if there were issues in their efficiency calibration. Considering both the large volume of affected literature and issues with reproducibility, it is difficult to assess and correct possible bias in many of these published works. This study demonstrates the importance of proper efficiency calibration and documentation in published work and can assist future experimentation and data analysis in avoiding bias introduced by the logarithmic polynomial formulation.

Acknowledgements

This work was supported by the US Nuclear Data Program at LBNL under contract DE-AC02-05CH11231 (LBNL), the Department of Energy National Nuclear Security Administration through the Nuclear Science and Security Consortium under Award Number DE-NA0003180, and the NNSA Graduate Fellowship Program. This work performed under the auspices of the U.S. Department of Energy by Lawrence Livermore National Laboratory under Contract DE-AC52-07NA27344. LLNL-JRNL-804061.

References

[1] Glenn G. Knoll, Radiation Detection and Measurement (4th Edition), John Wiley & Sons, Inc., 2010.

[2] G. L. Molnár, Z. Révay, T. Belgya, Wide energy range efficiency calibration method for Ge detectors, Nuclear Instruments and Methods in Physics Research, Section A: Accelerators, Spectrometers, Detectors and Associated Equipment 489 (1-3) (2002) 140–159. `doi:10.1016/S0168-9002(02)00902-6`.

[3] C. M. Baglin, E. Browne, E. B. Norman, G. L. Molnár, T. Belgya, Z. Révay, F. Szelecsényi, 66Ga: A standard for high-energy calibration of Ge detectors, Nuclear Instruments and Methods in Physics Research, Section A: Accelerators, Spectrometers, Detectors and Associated Equipment 481 (1-3) (2002) 365–377. `doi:10.1016/S0168-9002(01)01376-6`.

[4] D. C. Radford, Notes on the use of the program gf3 (2000).
URL `https://radware.phy.ornl.gov/gf3/`

[5] M. J. Koskelo, P. A. Aarnio, J. T. Routti, SAMPO80: An accurate gamma spectrum analysis method for minicomputers, Nuclear Instruments and Methods`doi:10.1016/0029-554X(81)90209-3`.

[6] P. A. Aarnio, M. T. Nikkinen, J. T. Routti, SAMPO 90 High resolution interactive gamma-spectrum analysis including automation with macros, Journal of Radioanalytical and Nuclear Chemistry Articles 160 (1) (1992) 289–295. `doi:10.1007/BF02041678`.

[7] J. Gunnink, R. and Niday, COMPUTERIZED QUANTITATIVE ANALYSIS BY GAMMA-RAY SPECTROMETRY. VOLUME I. DESCRIPTION OF THE GAMANAL PROGRAM`doi:10.2172/4696896`.

[8] M. Heimlich, P. A. Beeley, J. A. Page, GAMANAL-PC: A program for gamma-ray spectrum analysis using a microcomputer, Journal of Radioanalytical and Nuclear Chemistry Articles 132 (2) (1989) 281–291. `doi:10.1007/BF02136087`.

[9] B. Fazekas, T. Belgya, L. Dabolczi, G. Molnár, A. Simonits, HYPERMET-PC: Program for automatic analysis of complex gamma-ray spectra, Journal of Trace and Microprobe Techniques 14 (1) (1996) 167–172.

[10] W. J. Gallagher, S. J. Cipolla, A model-based efficiency calibration of a Si(Li) detector in the energy region from 3 to 140 keV, Nuclear Instruments and Methods 122 (C) (1974) 405–414. `doi:10.1016/0029-554X(74)90508-4`.

[11] R. Storn, K. Price, Differential Evolution - A Simple and Efficient Heuristic for Global Optimization over Continuous Spaces, Journal of Global Optimization`doi:10.1023/A:1008202821328`.

[12] P. P. Eric Jones, Travis Oliphant, SciPy: Open source scientific tools for Python.
URL `http://www.scipy.org/`

[13] D. Karamanis, V. Lacoste, S. Andriamonje, G. Barreau, M. Petit, Experimental and simulated efficiency of a HPGe detector with point-like and extended sources, Nuclear Instruments and Methods in Physics Research, Section A: Accelerators, Spectrometers, Detectors and Associated Equipment 487 (3) (2002) 477–487. `doi:10.1016/S0168-9002(02)00393-5`.

[14] A. Pastore, An introduction to bootstrap for nuclear physics, Journal of Physics G: Nuclear and Particle Physics 46 (5). arXiv:1810.05585, doi:10.1088/1361-6471/ab00ad.

[15] E. F. Matthews, Repository of reproducible workflow for significance of gamma-ray detector efficiency calibration bias on nuclear astrophysics and nuclear data evaluations (2019). doi:10.5281/zenodo.3579556.
URL https://mybinder.org/v2/zenodo/10.5281/zenodo.3579556/?filepath=Analysis.ipynb

[16] J. Fox, Applied regression analysis and generalized linear models, SAGE Publications, Inc., 2008.

[17] S. Raman, C. Yonezawa, H. Matsue, H. Iimura, N. Shinohara, Efficiency calibration of a Ge detector in the 0.1-11.0 MeV region, Nuclear Instruments and Methods in Physics Research, Section A: Accelerators, Spectrometers, Detectors and Associated Equipment 454 (2-3) (2000) 389–402. doi:10.1016/S0168-9002(00)00493-9.

[18] Z. Elekes, T. Belgya, G. L. Molnár, Á. Z. Kiss, M. Csatlós, J. Gulyás, A. Krasznahorkay, Z. Máté, Absolute full-energy peak efficiency calibration of a Clover-BGO detector system, Nuclear Instruments and Methods in Physics Research, Section A: Accelerators, Spectrometers, Detectors and Associated Equipment 503 (3) (2003) 580–588. doi:10.1016/S0168-9002(03)00998-7.

[19] T. Belgya, Improved accuracy of γ-ray intensities from basic principles for the calibration reaction N14(n,γ)N15, Physical Review C - Nuclear Physics 74 (2). doi:10.1103/PhysRevC.74.024603.

[20] G. L. Molnár, Z. Révay, R. L. Paul, R. M. Lindstrom, Prompt-gamma activation analysis using the k0 approach, Journal of Radioanalytical and Nuclear Chemistry 234 (1-2) (1998) 21–26. doi:10.1007/BF02389741.

[21] Z. Révay, T. Belgya, G. L. Molnár, Application of hypermet-PC in PGAA, Journal of Radioanalytical and Nuclear Chemistry 265 (2) (2005) 261–265. doi:10.1007/s10967-005-0818-2.

[22] H. Matsue, C. Yonezawa, k0 Standardization approach in neutron-induced prompt gamma-ray analysis at JAERI, Journal of Radioanalytical and Nuclear Chemistry 245 (1) (2000) 189–194.

[23] Z. Kasztovszky, Z. Rcvay, T. Belgya, B. Fazekas, J. Östör, G. L. Molnár, G. Molnár, J. Borossay, Investigation of impurities in thermoluminescent A12O3 materials by prompt-gamma activation analysis, Journal of Analytical Atomic Spectrometry 14 (4) (1999) 593–596. doi:10.1039/A808857H.

[24] D. Turkoglu, H. Chen-Mayer, R. Paul, R. Zeisler, Assessment of PGAA capability for low-level measurements of H in Ti alloys, Analystdoi:10.1039/c7an01308f.

[25] I. Salma, É. Zemplén-Papp, Instrumental neutron activation analysis for studying size-fractionated aerosols, Nuclear Instruments and Methods in Physics Research, Section A: Accelerators, Spectrometers, Detectors and Associated Equipment 435 (3) (1999) 462–474. doi:10.1016/S0168-9002(99)00654-3.

[26] A. Borella, T. Belgya, S. Kopecky, F. Gunsing, M. Moxon, M. Rejmund, P. Schillebeeckx, L. Szentmiklósi, Determination of the ^{209}Bi(n,γ)^{210}Bi and ^{209}Bi(n,γ)^{210m,g}Bi reaction cross sections in a cold neutron beam, Nuclear Physics A 850 (1) (2011) 1–21. doi:10.1016/j.nuclphysa.2010.11.006.
URL http://dx.doi.org/10.1016/j.nuclphysa.2010.11.006

[27] A. M. Hurst, R. B. Firestone, L. Szentmiklósi, B. W. Sleaford, M. S. Basunia, T. Belgya, J. E. Escher, M. Krtička, Z. Révay, N. C. Summers, Radiative thermal neutron-capture cross sections for the ^{180}W(n,γ) reaction and determination of the neutron-separation energy, Physical Review C - Nuclear Physics 92 (3). doi:10.1103/PhysRevC.92.034615.

[28] P. Schillebeeckx, T. Belgya, A. Borella, S. Kopecky, A. Mengoni, C. R. Quétel, L. Szentmiklósi, I. Trešl, R. Wynants, Neutron capture studies of 206Pb at a cold neutron beam, European Physical Journal A 49 (11) (2013) 1–8. doi:10.1140/epja/i2013-13143-3.

[29] T. H. Randriamalala, M. Rossbach, E. Mauerhofer, Z. Révay, S. Söllradl, F. M. Wagner, FaNGaS: A new instrument for (n,nγ) reaction measurements at FRM II, Nuclear Instruments and Methods in Physics Research, Section A: Accelerators, Spectrometers, Detectors and Associated Equipment 806 (2016) 370–377. doi:10.1016/j.nima.2015.10.026.

[30] C. Genreith, Partial Neutron Capture Cross Sections of Actinides using Cold Neutron Prompt Gamma Activation Analysis, Vol. 250, Jülich Forschungzentrum.

[31] A. Simonits, J. Östör, S. Kálvin, B. Fazekas, HyperLab: A new concept in gamma-ray spectrum analysis, Journal of Radioanalytical and Nuclear Chemistry 257 (3) (2003) 589–595. doi:10.1023/A:1025400917620.

[32] C. S. Park, H. D. Choi, G. M. Sun, J. H. Whang, Status of developing HPGe γ-ray spectrum analysis code HYPERGAM, Progress in Nuclear Energy 50 (2-6) (2008) 389–393. doi:10.1016/j.pnucene.2007.11.022.

[33] R. G. Helmer, N. Nica, J. C. Hardy, V. E. Iacob, Precise efficiency calibration of an HPGe detector up to 3.5 MeV, with measurements and Monte Carlo calculations, Applied Radiation and Isotopes 60 (2-4) (2004) 173–177. doi:10.1016/j.apradiso.2003.11.012.

[34] A. Favalli, H. C. Mehner, F. Simonelli, Wide energy range efficiency calibration for a lanthanum bromide scintillation detector, Radiation Measurementsdoi:10.1016/j.radmeas.2007.11.062.

[35] T. Belgya, New gamma-ray intensities for the 14N(n,γ)15N high energy standard and its influence on PGAA and on nuclear quantities, Journal of Radioanalytical and Nuclear Chemistry 276 (3) (2008) 609–614. doi:10.1007/s10967-008-0607-9.

[36] B. Blank, J. Souin, P. Ascher, L. Audirac, G. Canchel, M. Gerbaux, S. Grévy, J. Giovinazzo, H. Guérin, T. K. Nieto, I. Matea, H. Bouzomita, P. Delahaye, G. F. Grinyer, J. C. Thomas, High-precision efficiency calibration of a high-purity co-axial germanium detector, Nuclear Instruments and Methods in Physics Research, Section A: Accelerators, Spectrometers, Detectors and Associated Equipment 776 (2015) 34–44. doi:10.1016/j.nima.2014.12.071.
URL http://dx.doi.org/10.1016/j.nima.2014.12.071

[37] R. G. Helmer, Modern tools for precise γ-ray spectrometry with Ge detectors, Nuclear Instruments and Methods in Physics Research, Section A: Accelerators, Spectrometers, Detectors and Associated Equipment 505 (1-2) (2003) 297–305. doi:10.1016/S0168-9002(03)01073-8.

[38] H. Sakane, H. Obayashi, A. Tojo, M. Shibata, K. Kawade, A. Taniguchi, Preparation of a liquid nitrogen target for measurement of γ-rays in the 14N(n, γ)15N reaction as an intensity standard in energy regions up to 11 MeV, Applied Radiation and Isotopes 63 (1) (2005) 131–135. doi:10.1016/j.apradiso.2005.01.018.

[39] G. W. Severin, L. D. Knutson, P. A. Voytas, E. A. George, Half-life of Ga66, Physical Review C - Nuclear Physics 82 (6). doi:10.1103/PhysRevC.82.067301.

[40] G. L. Molnár, Z. Révay, T. Belgya, New Intensities for High Energy Gamma-ray Standards, in: Capture Gamma-Ray Spectroscopy and Related Topics, 2003, pp. 522—-530. doi:10.1142/9789812795151_0067.

[41] I. Miyazaki, H. Sakane, H. Takayama, M. Kasaishi, A. Tojo, M. Furuta, H. Hayashi, O. Suematsu, H. Narasaki, T. Shimizu, M. Shibata, K. Kawade, A. Taniguchi, H. Harada, Precise intensity measurements in the14N(n, γ)15N reaction as a γ-ray intensity standard up to 11MeV, Journal of Nuclear Science and Technology 45 (6) (2008) 481–486. doi:10.1080/18811248.2008.9711871.

[42] K. S. Krane, The decays of 70,72Ga to levels of 70,72Ge and the neutron capture cross sections of 69,71Ga, Applied Radiation and Isotopes 70 (8) (2012) 1649–1657. doi:10.1016/j.apradiso.2012.04.008.
URL http://dx.doi.org/10.1016/j.apradiso.2012.04.008

[43] K. S. Krane, Neutron capture by 94,96Zr and the decays of 97Zr and 97Nb, Applied Radiation and Isotopes 94 (2014)

60–66. doi:10.1016/j.apradiso.2014.07.006.
URL http://dx.doi.org/10.1016/j.apradiso.2014.07.006

[44] K. S. Krane, M. L. Keck, E. B. Norman, A. P. Shivprasad, Gamma-ray energies in the decay of 38Cl, Applied Radiation and Isotopes 70 (4) (2012) 740–742. doi:10.1016/j.apradiso.2011.12.033.
URL http://dx.doi.org/10.1016/j.apradiso.2011.12.033

[45] P. Dryak, P. Kovar, Determination of emission probabilities of gamma photons in the decay of 56Co, Applied Radiation and Isotopes 66 (6-7) (2008) 711–714. doi:10.1016/j.apradiso.2008.02.008.

[46] K. S. Krane, Gamma-ray spectroscopy in the decay of 83Se to levels of 83Br, Applied Radiation and Isotopes 97 (2015) 12–20. doi:10.1016/j.apradiso.2014.12.006.
URL http://dx.doi.org/10.1016/j.apradiso.2014.12.006

[47] W. Urban, M. Jentschel, B. Märkisch, T. Materna, C. Bernards, C. Drescher, C. Fransen, J. Jolie, U. Köster, P. Mutti, T. Rzca-Urban, G. S. Simpson, New instrumentation for precise (n,γ) measurements at ILL Grenoble, Journal of Instrumentation 8 (3). doi:10.1088/1748-0221/8/03/P03014.

[48] G. L. Molnár, T. Belgya, Z. Révay, S. M. Qaim, Partial and total thermal neutron capture cross sections for non-destructive assay and transmutation monitoring of 99Tc, Radiochimica Acta 90 (8) (2002) 479–482. doi:10.1524/ract.2002.90.8_2002.479.

[49] M. U. Khandaker, H. Haba, M. Murakami, N. Otuka, Production cross-sections of long-lived radionuclides in deuteron-induced reactions on natural zinc up to 23 MeV, Nuclear Instruments and Methods in Physics Research, Section B: Beam Interactions with Materials and Atoms 346 (2015) 8–16. doi:10.1016/j.nimb.2015.01.011.
URL http://dx.doi.org/10.1016/j.nimb.2015.01.011

[50] E. Browne, J. Tuli, Nuclear Data Sheets for A = 66, Nuclear Data Sheets 111 (2010) 1093—-1209. doi:10.1016/j.nds.2010.03.004.
URL 10.1016/j.nds.2010.03.004

[51] A. L. Nichols, IAEA Co-ordinated Research Project: Update of X-ray and γ-ray decay data standards for detector calibration and other applications, Applied Radiation and Isotopes 60 (2-4) (2004) 247–256. doi:10.1016/j.apradiso.2003.11.025.

[52] M. Sabet, P. Rowshanfarzad, A. R. Jalilian, M. R. Ensaf, A. A. Rajamand, Production and quality control of66Ga radionuclide, Nukleonika 51 (3) (2006) 147–154.

[53] P. Rowshanfarzad, A. R. Jalilian, M. Sabet, M. Akhlaghi, Production and quality control of ^{66}Ga as a PET radioisotope, Iranian Journal of Radiation Research 2 (3) (2004) 149–158.

[54] Y. Xu, K. Takahashi, S. Goriely, M. Arnould, M. Ohta, H. Utsunomiya, NACRE II: An update of the NACRE compilation of charged-particle-induced thermonuclear reaction rates for nuclei with mass number A $>$ 16, Nuclear Physics A 918 (2013) 61–169. arXiv:1310.7099, doi:10.1016/j.nuclphysa.2013.09.007.

[55] A. Redder, H. W. Becker, C. Rolfs, H. P. Trautvetter, T. R. Donoghue, T. C. Rinckel, J. W. Hammer, K. Langanke, The ^{12}C(α, γ)^{16}O cross section at stellar energies, Nuclear Physics, Section A 462 (2) (1987) 385–412. doi:10.1016/0375-9474(87)90555-0.

[56] J. M. Ouellet, M. N. Butler, H. C. Evans, H. W. Lee, J. R. Leslie, J. D. MacArthur, W. McLatchie, H. B. Mak, P. Skensved, J. L. Whitton, X. Zhao, T. K. Alexander, 12C(α,γ)16O cross sections at stellar energies, Physical Review C - Nuclear Physics 54 (4) (1996) 1982–1998. doi:10.1103/PhysRevC.54.1982.

[57] G. Roters, C. Rolfs, F. Strieder, H. P. Trautvetter, The E1 and E2 capture amplitudes in 12C(α,γ0)16O, European Physical Journal A 6 (4) (1999) 451–461. doi:10.1007/s100500050369.

[58] L. Gialanella, D. Rogalla, F. Strieder, S. Theis, G. Gyürki, C. Agodi, R. Alba, M. Aliotta, L. Campajola, A. Del Zoppo, A. D'Onofrio, P. Figuera, U. Greife, G. Imbriani, A. Ordine, V. Roca, C. Rolfs, M. Romano, C. Sabbarese, P. Sapienza, F. Schümann, E. Somorjai, F. Terrasi, H. P. Trautvetter, The E1 capture amplitude in 12C(α, γ0)16O, European Physical Journal A 11 (3) (2001) 357–370. doi:10.1007/s100500170075.

[59] R. Kunz, M. Jaeger, A. Mayer, J. W. Hammer, G. Staudt, S. Harissopulos, T. Paradellis, 12C(α, γ)16O: The key reaction in stellar nucleosynthesis, Physical Review Letters 86 (15) (2001) 3244–3247. doi:10.1103/PhysRevLett.86.3244.

[60] M. Fey, Im Brennpunkt der Nuklearen Astrophysik : Die Reaktion ^{12}C(α,γ)^{16}Odoi:10.18419/opus-4716.

[61] M. Assunção, M. Fey, A. Lefebvre-Schuhl, J. Kiener, V. Tatischeff, J. W. Hammer, C. Beck, C. Boukari-Pelissie, A. Coc, J. J. Correia, S. Courtin, F. Fleurot, E. Galanopoulos, C. Grama, F. Haas, F. Hammache, F. Hannachi, S. Harissopulos, A. Korichi, R. Kunz, D. Ledu, A. Lopez-Martens, D. Malcherek, R. Meunier, T. Paradellis, M. Rousseau, N. Rowley, G. Staudt, S. Szilner, J. P. Thibaud, J. L. Weil, E1 and E2S factors of C12(α,γ0)O16 from γ-ray angular distributions with a 4 π-detector array, Physical Review C - Nuclear Physics 73 (5) (2006) 1–19. doi:10.1103/PhysRevC.73.055801.

[62] R. W. Kunz, Die Schlüsselreaktion im Heliumbrennen der Sternedoi:10.18419/opus-4689.

[63] P. Dyer, C. A. Barnes, The 12C(α, γ)16O reaction and stellar helium burning, Nuclear Physics, Section A 233 (2) (1974) 495–520. doi:10.1016/0375-9474(74)90470-9.

[64] R. M. Kremer, C. A. Barnes, K. H. Chang, H. C. Evans, B. W. Filippone, K. H. Hahn, L. W. Mitchell, Coincidence measurement of the 12C(,)16O cross section at low energies, Physical Review Letters 60 (15) (1988) 1475–1478. doi:10.1103/PhysRevLett.60.1475.

[65] H. Makii, Y. Nagai, T. Shima, M. Segawa, K. Mishima, H. Ueda, M. Igashira, T. Ohsaki, E1 and E2 cross sections of the C12(α,γ0)O16 reaction using pulsed α beams, Physical Review C - Nuclear Physics 80 (6). doi:10.1103/PhysRevC.80.065802.

[66] D. Schürmann, A. Di Leva, L. Gialanella, R. Kunz, F. Strieder, N. De Cesare, M. De Cesare, A. D'Onofrio, K. Fortak, G. Imbriani, D. Rogalla, M. Romano, F. Terrasi, Stuy of the 6.05 MeV cascade transition in 12C(α,γ)16O, Physics Letters, Section B: Nuclear, Elementary Particle and High-Energy Physics 703 (5) (2011) 557–561. doi:10.1016/j.physletb.2011.08.061.
URL http://dx.doi.org/10.1016/j.physletb.2011.08.061

[67] K. U. Kettner, H. W. Becker, L. Buchmann, C. Rolls, P. Schmalbrock, H. P. Trautvetter, A. Vlieks, the 4He(12C,gamma)16O reaction at stellar energies, Z. Phys. A. - Atoms and Nuclei 94 (1982) 73–94.

[68] R. Plag, R. Reifarth, M. Heil, F. Käppeler, G. Rupp, F. Voss, K. Wisshak, 12C(α,γ)16O studied with the Karlsruhe 4π BaF2 detector, Physical Review C - Nuclear Physics 86 (1) (2012) 1–9. doi:10.1103/PhysRevC.86.015805.

[69] C. Matei, L. Buchmann, W. R. Hannes, D. A. Hutcheon, C. Ruiz, C. R. Brune, J. Caggiano, A. A. Chen, J. D'Auria, A. Laird, M. Lamey, Z. Li, W. Liu, A. Olin, D. Ottewell, J. Pearson, G. Ruprecht, M. Trinczek, C. Vockenhuber, C. Wrede, Measurement of the cascade transition via the first excited state of O16 in the C12(α,γ)O16 reaction, and its S factor in stellar helium burning, Physical Review Letters 97 (24) (2006) 1–4. doi:10.1103/PhysRevLett.97.242503.